

# Interplay of $\gamma$ -Rigid and $\gamma$ -Stable Collective Motion in Neutron Rich Rare Earth Nuclei

R. Budaca, A.I. Budaca

National Institute of Physics and Nuclear Engineering, 077125, Romania

Received 9 October 2015

**Abstract.** A simple exactly separable version of the Bohr Hamiltonian which combines the  $\gamma$ -stable and  $\gamma$ -rigid collective motion is used to describe few neutron rich rare earth nuclei. The coupling between the two types of collective motion is managed through a rigidity parameter. Considering a potential of the form  $u(\beta) + v(\gamma)/\beta^2$  adapted to the current problem and restricting the  $\gamma$ -stable part of the Hamiltonian to stiff oscillations around the  $\gamma$  value of the rigid motion one obtains an exact separation of variables. Moreover, the separated potential for  $\beta$  variable is chosen such that in the lower limit of the rigidity parameter, the model recovers exactly the ES- $X(5)$  or ES-D solutions, while in the upper limit it tends to the prolate  $\gamma$ -rigid solutions  $X(3)$  or  $X(3)$ -D. The experimental realization of the model is found in few transitional rare earth nuclei around  $N = 96$  where a singular behaviour is observed.

PACS codes: 21.60.Ev, 21.10.Re, 27.70.+q

## 1 Introduction

The introduction of the Algebraic Collective Model [1] which allows a rapidly converging diagonalization procedure for solving the Bohr Hamiltonian for any general potential and the near exhaustion of the exactly and approximatively solvable potentials, impinged the search for alternative approaches to describe collective phenomena. A promising direction in this sense is represented by the realization of the Bohr-Mottelson model in other than the usual five-dimensional shape phase space. Indeed, while the reformulation of the Bohr Hamiltonian in six dimensions [2] explains the origin of the deformation dependent mass term [3, 4], the  $\gamma$ -rigid regimes lead to simple descriptions of the basic rotation-vibration coupling with good agreement with experiment [5–12]. The obvious theoretical similarities between the  $\gamma$ -rigid and  $\gamma$ -stable hypotheses regarding the quadrupole collective excitations, inspired a hybrid model based on the interplay between these two already well established approaches [13]. The idea is basically to combine the  $\gamma$ -rigid prolate picture with an additional stiff  $\gamma$  oscillation around  $\gamma = 0$  through a  $\gamma$ -rigidity control parameter which acts as a

weighting measure for the corresponding kinetic operators. The formalism was firstly used in combination with an infinite square well (ISW) potential for the  $\beta$  variable [13], and recently extrapolated to the Davidson (D) potential [14]. The last being more pliable, revealed a singular behaviour for the  $N = 96$  isotopes of Gd and Dy compared to their neighbours.

## 2 $\gamma$ -Stable/Rigid Collective Hamiltonian

The description of a combined  $\gamma$ -rigid and  $\gamma$ -soft nucleus was approached by considering the Hamiltonian [13, 14]

$$H = \chi \hat{T}_r + (1 - \chi) \hat{T}_s + V(\beta, \gamma), \quad (1)$$

where  $0 \leq \chi < 1$  measures the system's  $\gamma$ -rigidity and

$$\hat{T}_r = -\frac{\hbar^2}{2B} \left[ \frac{1}{\beta^2} \frac{\partial}{\partial \beta} \beta^2 \frac{\partial}{\partial \beta} - \frac{\mathbf{Q}^2}{3\beta^2} \right] \quad (2)$$

being the  $\gamma$ -rigid kinetic energy operator, while

$$\hat{T}_s = -\frac{\hbar^2}{2B} \left[ \frac{1}{\beta^4} \frac{\partial}{\partial \beta} \beta^4 \frac{\partial}{\partial \beta} + \frac{1}{\beta^2 \sin 3\gamma} \frac{\partial}{\partial \gamma} \sin 3\gamma \frac{\partial}{\partial \gamma} - \frac{1}{4\beta^2} \sum_{k=1}^3 \frac{Q_k^2}{\sin^2(\gamma - \frac{2}{3}\pi k)} \right] \quad (3)$$

is its usual expression from the five dimensional Bohr Hamiltonian.  $\mathbf{Q}$  is the angular momentum operator from the intrinsic frame of reference and  $Q_k$  ( $k = 1, 2, 3$ ) denote the operators of its corresponding projections. The exact separation of the  $\beta$  variable from the  $\gamma$ -angular ones is achieved by considering the following expression for the potential energy:

$$v(\beta, \gamma) = \frac{2B}{\hbar^2} V(\beta, \gamma) = u(\beta) + (1 - \chi) \frac{v(\gamma)}{\beta^2}. \quad (4)$$

Factorizing the total wave function as  $\Psi(\beta, \gamma, \Omega) = \xi(\beta)\eta(\gamma)D_{MK}^L(\Omega)$  where  $D_{MK}^L$  are the Wigner functions with  $\Omega$  denoting the set of three Euler angles and  $L$  being the total angular momentum, while  $M$  and  $K$  - its projections on the body-fixed and respectively laboratory-fixed z axis, the associated Schrödinger equation is separated into a  $\beta$  part

$$\left[ -\frac{\partial^2}{\partial \beta^2} - \frac{4}{\beta} \frac{\partial}{\partial \beta} + \frac{W}{\beta^2} + u(\beta) \right] \xi(\beta) = \epsilon \xi(\beta), \quad (5)$$

where  $\epsilon = \frac{2B}{\hbar^2} E$ , and a  $\gamma$ -angular one. The last one is averaged on the Wigner states and treated further in the small angle approximation. The  $\gamma$  potential is

*Interplay of  $\gamma$ -Rigid and  $\gamma$ -Stable Collective Motion in ...*

chosen of the  $\gamma$ -stable form  $v(\gamma) = (3a)^2 \frac{\gamma^2}{2}$ , such that the associated  $\gamma$  solution is readily obtained

$$\eta_{n_\gamma K}(\gamma) = N_{n_\gamma K} \gamma^{|\frac{K}{2}|} e^{-3a \frac{\gamma^2}{2}} L_n^{|\frac{K}{2}|}(3a\gamma^2), \quad (6)$$

where  $N_{n_\gamma K}$  is a normalization constant,  $n = (n_\gamma - |K|/2)/2$  and  $a$  is a parameter associated through the string constant of the harmonic oscillator potential to the stiffness of  $\gamma$  vibrations. With this, the coupling constant  $W$  is given as

$$W = \frac{L(L+1) - (1-\chi)K^2}{3} + (1-\chi)a(n_\gamma + 1). \quad (7)$$

In what concerns the  $\beta$  equation, it is solved here for two potentials, namely the infinite square well [13]

$$u^{ISW}(\beta) = \begin{cases} 0, & \beta \leq \beta_W, \\ \infty, & \beta > \beta_W, \end{cases} \quad (8)$$

and Davidson [14]

$$u^D(\beta) = \beta^2 + \frac{\beta_0^4}{\beta^2}. \quad (9)$$

The corresponding solutions are given in terms of Bessel functions and associated Laguerre polynomials:

$$\xi_{LK n_\beta n_\gamma}^{ISW}(\beta) = N_{n_\beta, \nu} \beta^{\chi - \frac{3}{2}} J_\nu(x_{n_\beta+1, \nu} \beta / \beta_W), \quad (10)$$

$$\xi_{LK n_\beta n_\gamma}^D(\beta) = N_{n_\beta p} \beta^{p+\chi} e^{-\frac{\beta^2}{2}} L_n^{p+\frac{3}{2}}(\beta^2), \quad (11)$$

while the resulting total energies of the system are given as

$$\epsilon_{LK n_\beta n_\gamma}^{ISW} = \left( \frac{x_{n_\beta+1, \nu}}{\beta_W} \right)^2, \quad (12)$$

$$\epsilon_{LK n_\beta n_\gamma}^D = 2n_\beta + p + \frac{5}{2}, \quad (13)$$

where  $x_{s, \nu}$  is the  $s$ -th zero of the Bessel function  $J_\nu(x_{s, \nu} \beta / \beta_W)$  and  $\nu = \sqrt{(p+3/2)^2 - \beta_0^4}$  with

$$p = -\frac{3}{2} + \left[ \frac{L(L+1) - (1-\chi)K^2}{3} + \beta_0^4 + \left( \frac{3}{2} - \chi \right)^2 + (1-\chi)3a(n_\gamma + 1) \right]^{\frac{1}{2}} \quad (14)$$

The normalisation constants from (10) and (11) are computed with the integration measure  $\beta^{4-2\chi} d\beta$ , whose  $\chi$  dependence can be explained by constructing a similar model from the classical picture. Indeed, in order to have an equivalence between the two approaches one must have a  $\chi$  dependent integration metric associated to the quantum Hamiltonian (1) [14]. In this way, depending on the considered  $\beta$  potential, the presented formalism reproduces the energy spectrum as well as the  $\beta$  density probability of the  $\gamma$ -stable models ES-X(5) [15] and ES-D [16] when  $\chi = 0$  and that of their  $\gamma$ -rigid counterparts X(3) [7] and respectively X(3)-D [14] when  $\chi \rightarrow 1$ .

### 3 Numerical Application

Excepting the scale, the model presented in the last section has two free parameters common to both solutions (ISW and D), namely the stiffness of the  $\gamma$  oscillations  $a$  and the control parameter  $\chi$  which measures the degree of the system's  $\gamma$ -rigidity. The use of a Davidson  $\beta$  potential introduces another parameter -  $\beta_0$  which gives the position of the potential's minimum. The effect of all these parameters on the energy spectrum is fully investigated in Refs. [13, 14].

The experimental realization of such ambiguous collective conditions was found to occur in Gd and Dy isotopes around  $N = 96$ . The  $N = 96$  isotopes were first pointed out in connection to the ISW  $\beta$  solution [13]. The use of the Davidson  $\beta$  potential, provides a more pliable model due to an additional parameter, such that the corresponding energy formula is able to describe not only the same  $N = 96$  isotopes but also their heavier and lighter neighbours. The selection of model's candidate nuclei was judged by the smallest values for the quantity

$$\sigma = \sqrt{\frac{1}{N-1} \sum_{i=1}^N \left[ \frac{E_i(Th)}{E_{2_g^+}(Th)} - \frac{E_i(Exp)}{E_{2_g^+}(Exp)} \right]^2}, \quad (15)$$

where  $E_i(Th)$  is the value calculated using either Eq.(12) or (13) and  $i$  goes over the states of all considered bands. As can be seen from Figure 1 where the results of the fitting procedure are graphically presented, the agreement with experiment for all treated nuclei is very good. Especially well are reproduced the ground and  $\gamma$  band energies, while the  $\beta$  band is the main origin of discrepancies. The energy spectra of Dy isotopes are overall better described. The resulting set of parameters from the fitting procedure given in Table 1 are further used to compute the ratios for some relevant  $B(E2)$  rates. Using the quadrupole transition operator

$$T_m^{(E2)} = tq_m, \quad (16)$$

Table 1. Parameters involved in (12) and (13) obtained by fitting the experimental data [18–21].

Nucleus	$v(\beta)$	$\chi$	$a$	$\beta_0$	$\sigma$
$^{158}\text{Gd}$	D	$3 \cdot 10^{-4}$	11.349	2.044	0.601
$^{160}\text{Gd}$	D	0.826	51.538	2.840	0.768
$^{160}\text{Gd}$	ISW	0.948	168.899	-	0.567
$^{162}\text{Gd}$	D	0.092	9.052	2.963	0.574
$^{160}\text{Dy}$	D	0.423	14.519	2.442	0.636
$^{162}\text{Dy}$	D	0.067	7.934	3.056	0.411
$^{162}\text{Dy}$	ISW	0.269	10.309	-	0.845
$^{164}\text{Dy}$	D	0.734	24.473	3.205	0.092

Interplay of  $\gamma$ -Rigid and  $\gamma$ -Stable Collective Motion in ...

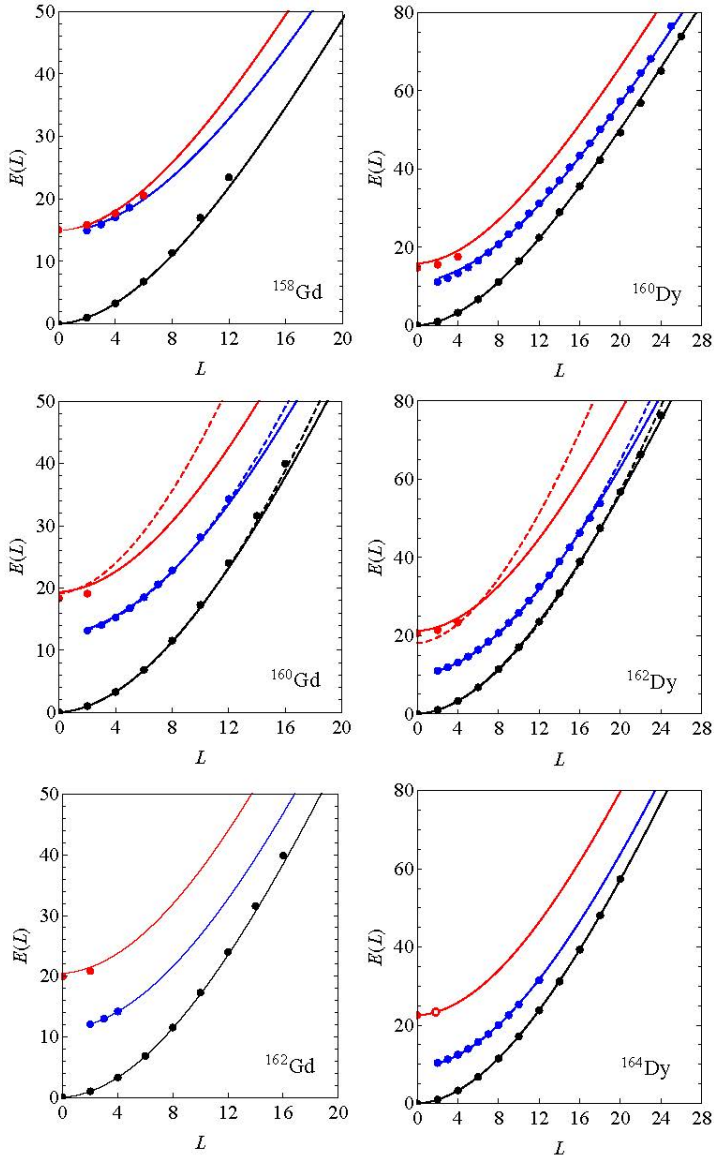


Figure 1. (Color online) Theoretical results for ground,  $\beta$  and  $\gamma$  bands energies normalized to the energy of the first excited state  $2_g^+$  are compared with the available experimental data for  $^{158-162}\text{Gd}$  [18–20] and  $^{160-164}\text{Dy}$  [19–21]. For  $N = 96$  nuclei the predictions with the ISW  $\beta$  potential are also shown. Open symbols indicate uncertain experimental data.

where  $t$  is a scaling factor and  $q_m$  is the quadrupole tensor, one can write the  $E2$  transition probability in the factorized form [16, 17]:

$$B(E2, LK n_{\beta} n_{\gamma} \rightarrow L' K' n'_{\beta} n'_{\gamma}) = \frac{5t^2}{16\pi} \left( C_{KK' - KK'}^{L 2 L'} B_{L' K' n'_{\beta} n'_{\gamma}}^{LK n_{\beta} n_{\gamma}} G_{K' n'_{\gamma}}^{K n_{\gamma}} \right)^2, \quad (17)$$

where  $B$  and  $G$  are integrals corresponding to the shape variables  $\beta$  and  $\gamma$  with the integration measures  $\beta^{4-2\chi} d\beta$  and respectively  $|\sin 3\gamma| d\gamma$ , while  $C$  is the Clebsch-Gordan coefficient resulting from the angular scalar product. Note that although here one uses the  $\chi$  dependent integration measure instead of the usual one used in Ref. [13], the correction have an almost negligible effect on the numerical values for most of the transitions. The theoretical results for the ground to ground transitions normalized to the  $B(E2, 2_g^+ \rightarrow 0_g^+)$  value are shown graphically in Figure 2 together with the available experimental data points, while those corresponding to low lying interband transitions are compared with scarce experimental values in Table 2. As the considered nuclei are generally accepted as being strongly deformed, the theoretical results are also compared

Table 2. Theoretical estimations of the ratios corresponding to few low lying interband  $B(E2)$  transition probabilities calculated with ISW for  $N = 96$  nuclei and with D potential for all considered nuclei are compared with available experimental data.  $\Delta K = 0$  transitions are normalized to the  $2_{\beta}^+ \rightarrow 0_g^+$  transition, while  $\Delta K = 2$  transitions to the  $2_{\gamma}^+ \rightarrow 0_g^+$  transition, as in Refs. [16, 17]. R.R. stands for Rigid Rotor.

Nucleus	$\frac{2_{\beta}^+ \rightarrow 2_g^+}{2_{\beta}^+ \rightarrow 0_g^+}$	$\frac{2_{\beta}^+ \rightarrow 4_g^+}{2_{\beta}^+ \rightarrow 0_g^+}$	$\frac{2_{\gamma}^+ \rightarrow 2_g^+}{2_{\gamma}^+ \rightarrow 0_g^+}$	$\frac{2_{\gamma}^+ \rightarrow 4_g^+}{2_{\gamma}^+ \rightarrow 0_g^+}$
<sup>158</sup> Gd	0.25(6)	4.48(75)	1.76(26)	0.079(14)
D	1.93	6.01	1.46	0.077
<sup>160</sup> Gd			1.87(12)	0.189(29)
D	1.79	4.97	1.44	0.074
ISW	1.81	5.00	1.45	0.074
<sup>162</sup> Gd				
D	1.76	4.80	1.44	0.074
<sup>160</sup> Dy		2.52(44)	1.89(18)	0.133(14)
D	1.89	5.70	1.45	0.075
<sup>162</sup> Dy			1.78(16)	0.137(12)
D	1.75	4.70	1.44	0.073
ISW	1.84	5.18	1.45	0.074
<sup>164</sup> Dy			2.00(27)	0.240(33)
D	1.73	4.55	1.44	0.073
R.R.	1.43	2.57	1.43	0.071

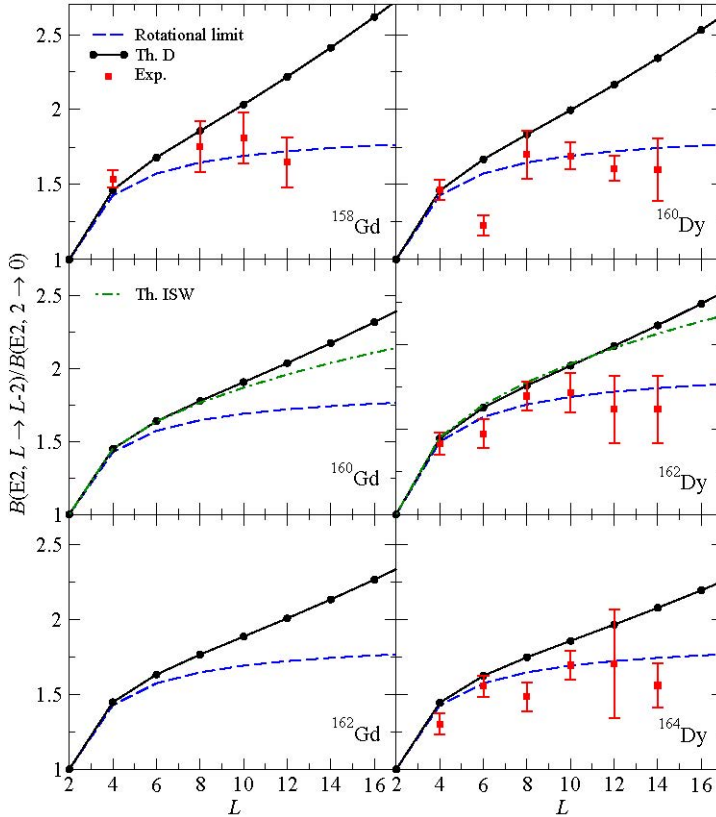


Figure 2. (Color online) Theoretical ground state to ground state  $E2$  transition probabilities normalized to the  $2_g^+ \rightarrow 0_g^+$  transition are compared with the available experimental data corresponding to all considered nuclei and with the rigid rotor predictions. For  $N = 96$  nuclei the predictions with the ISW  $\beta$  potential are also shown.

with the rigid rotor predictions. In this context the experimental points from Figure 2 are situated generally in between the rigid rotor and present model's predictions.

The numerical values of the fitted rigidity parameter  $\chi$  reveal a singular behaviour of the  $N = 96$  nuclei in respect to their neighbours. Indeed, while  $^{160}\text{Gd}$  exhibits a high  $\gamma$ -rigidity, its neighbours are more of the  $\gamma$ -stable type. The same happens with the  $^{160}\text{Gd}$  isotope in regard to the  $\gamma$ -rigidity of its neighbours but less strikingly and with an opposite effect, i.e.  $^{162}\text{Dy}$  nucleus is near  $\gamma$ -stable whereas its neighbours exhibit a fair amount of  $\gamma$ -rigid/stable mixing. From the present model's point of view there is definitely a critical aspect in the behaviour of the  $^{160}\text{Gd}$  and  $^{162}\text{Dy}$  nuclei, which is also supported by the fact that these nuclei were also well described with the maximally anharmonic shape of

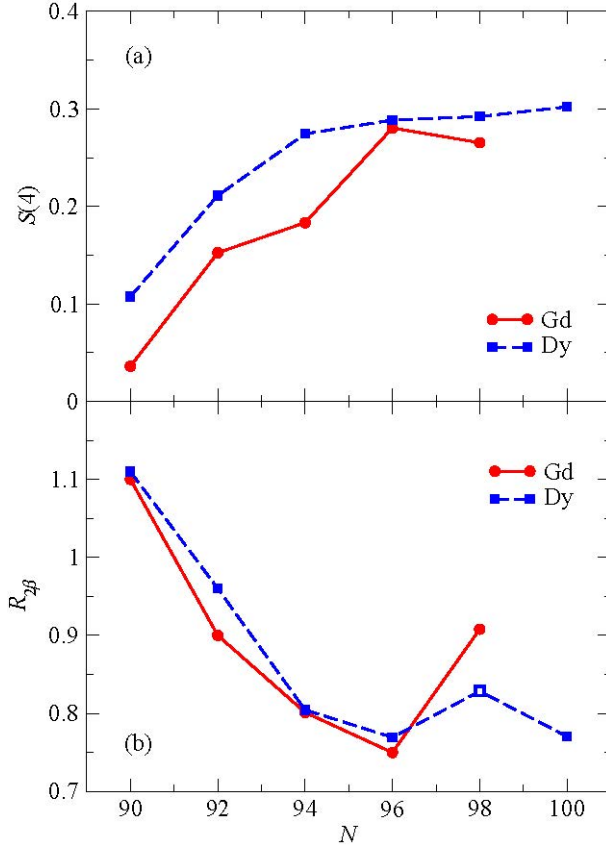


Figure 3. (Color online)  $S(4)$  (a) and  $R_{2\beta}$  (b) quantities as function of the neutron number  $N$  for the Gd and Dy isotopic chains, calculated using the experimental energies from Refs. [18–23]. The open symbol corresponds to a value calculated using uncertain experimental data.

the  $\beta$  potential, i.e. ISW. In order to find some experimental evidence for such a singularity in  $N = 96$  nuclei of the Gd and Dy isotopic chains, one plotted in Figure 3 as function of the neutron number  $N$ , the following quantities:

$$S(4) = \frac{[E(4_{\gamma}^+) - E(3_{\gamma}^+)] - [E(3_{\gamma}^+) - E(2_{\gamma}^+)]}{E(2_g^+)}, \quad (18)$$

$$R_{2\beta} = \frac{E(2_{\beta}^+) - E(0_{\beta}^+)}{E(2_g^+)}. \quad (19)$$

which are calculated with experimental data and describe the  $\gamma$ -band staggering [24] and the relative spacing of the lowest states in the  $\beta$  excited band [16],

respectively. In the first case a local peak is registered at  $N = 96$  which is sharper for the Gd chain in comparison to the Dy isotopes where it is barely visible, while in the latter case both chains have clear minima at  $N = 96$  and once again the minimum is sharper for the Gd chain. However, these spectral signatures do not hint to the opposite effect found in relation to the  $\gamma$ -rigidity parameter values of Gd and Dy isotopes. An experimental validation of this distinction can be seen in Table 2 where the experimental values of the  $B(E2, 2_{\gamma}^+ \rightarrow 2_g^+)/B(E2, 2_{\gamma}^+ \rightarrow 0_g^+)$  ratio for the  $^{160}\text{Dy}$  nucleus is smaller than that of its neighboring isotopes, while the same ratio corresponding to  $^{160}\text{Gd}$  have a greater value than its lighter isotope.

#### **4 Conclusions**

A simple exactly separable model was presented which considers the kinetic energy of the Bohr Hamiltonian as a combination of prolate  $\gamma$ -rigid and  $\gamma$ -stable rotation-vibration kinetic operators. The relative strength of these two components is managed through a so called rigidity parameter. This parameter serves as a weighting measure which bridges the  $X(3)$  and  $X(3)$ -D  $\gamma$ -rigid solutions to their  $\gamma$ -stable realisations represented by ES- $X(5)$  and ES-D models when an ISW potential and respectively a Davidson potential in the  $\beta$  shape variable are adopted. Resulting models with ISW and Davidson  $\beta$  potentials contain two and respectively three free parameters excepting the scale, which are used to fit experimental data and ultimately select the model's candidates. The best experimental realization of the model with ISW is found in few rare earth nuclei with  $N = 96$ , namely  $^{160}\text{Gd}$  and  $^{162}\text{Dy}$ . Using the Davidson potential enables the description also of their lighter and heavier neighboring isotopes which present quite distinct features in what concerns the  $\gamma$ -rigid/stable mixing. For all considered nuclei a very good agreement is obtained with experimental energy spectrum and available  $E2$  transition probabilities. The occurrence of  $^{160}\text{Gd}$  and  $^{162}\text{Dy}$  as singular points in their respective isotopic chains due to abnormal collective behaviour is also discussed for the first time in terms of some experimental spectral and electromagnetic signatures.

In conclusion, the proposed hybrid formalism unveils alternative features of the collective motion in the vicinity of the critical point of a spherical to deformed shape phase transition and represents an important step in the understanding of the evolution of collectivity in the neutron rich transitional nuclei.

#### **Acknowledgments**

Support received from the Romanian Ministry of Education and Research through the Project PN-09-37-01-02/2013 is gratefully acknowledged.

## References

- [1] D.J. Rowe (2004) *Nucl. Phys. A* **735** 372.
- [2] P.E. Georgoudis (2014) *Phys. Lett. B* **731** 122.
- [3] D. Bonatsos, P.E. Georgoudis, D. Lenis, N. Minkov, and C. Quesne (2011) *Phys. Rev. C* **83** 044321.
- [4] D. Bonatsos, P.E. Georgoudis, N. Minkov, D. Petrellis, and C. Quesne (2013) *Phys. Rev. C* **88** 034316.
- [5] A.S. Davydov and A.A. Chaban (1960) *Nucl. Phys.* **20** 499.
- [6] D. Bonatsos, D. Lenis, D. Petrellis, P.A. Terziev, and I. Yigitoglu (2005) *Phys. Lett. B* **621** 102.
- [7] D. Bonatsos, D. Lenis, D. Petrellis, P.A. Terziev, and I. Yigitoglu (2006) *Phys. Lett. B* **632** 238.
- [8] R. Budaca (2014) *Eur. Phys. J. A* **50** 87.
- [9] R. Budaca (2014) *Phys. Lett. B* **739** 86.
- [10] P. Buganu and R. Budaca (2015) *Phys. Rev. C* **91** 014306.
- [11] P. Buganu and R. Budaca (2015) *J. Phys. G: Nucl. Part. Phys.* **42** 105106.
- [12] Yu Zhang, Feng Pan, Yan-An Luo, Yu-Xin Liu, and J. P. Draayer (2012) *Phys. Rev. C* **86** 044312.
- [13] R. Budaca and A.I. Budaca (2015) *J. Phys. G: Nucl. Part. Phys.* **42** 085103.
- [14] R. Budaca and A.I. Budaca (2015) *Eur. Phys. J. A* **51** 126.
- [15] D. Bonatsos, D. Lenis, E.A. McCutchan, D. Petrellis, and I. Yigitoglu (2007) *Phys. Lett. B* **649** 394.
- [16] D. Bonatsos *et al.* (2007) *Phys. Rev. C* **76** 064312.
- [17] R. Bijker, R.F. Casten, N.V. Zamfir, and E.A. McCutchan (2003) *Phys. Rev. C* **68** 064304.
- [18] R.G. Helmer (2004) *Nucl. Data Sheets* **101** 325.
- [19] C.W. Reich (2005) *Nucl. Data Sheets* **105** 557.
- [20] C.W. Reich (2007) *Nucl. Data Sheets* **108** 1807.
- [21] Balraj Singh (2001) *Nucl. Data Sheets* **93** 243.
- [22] C.M. Baglin (2008) *Nucl. Data Sheets* **109** 1103.
- [23] C.M. Baglin (2010) *Nucl. Data Sheets* **111** 1807.
- [24] N.V. Zamfir and R.F. Casten (1991) *Phys. Lett. B* **260** 265.
- [25] F. Iachello and A. Arima (1978) *The Interacting Boson Model*, Cambridge University Press, Cambridge.